Applied Catalysis B: Environmental 188 (2016) 113–122

Contents lists available at ScienceDirect

Applied Catalysis B: Environmental

journal homepage: www.elsevier.com/locate/apcatb

Fe_3O_4@β-CD nanocomposite as heterogeneous Fenton-like catalyst for enhanced degradation of 4-chlorophenol (4-CP)

Manlin Wang[a,1], Guodong Fang[b,1], Peng Liu[a,c], Dongmei Zhou[b], Chen Ma[a], Dongju Zhang[a], Jinhua Zhan[a,*]

[a] Key Laboratory for Colloid & Interface Chemistry of Education Ministry, Department of Chemistry, Shandong University, Jinan 250100, PR China
[b] Key Laboratory of Soil Environment and Pollution Remediation, Institute of Soil Science, Chinese Academy of Sciences, 71 East Beijing Road, Nanjing 210008, PR China
[c] School of Chemistry and Chemical Engineering, Qvfu Normal University, Qvfu 273165, PR China

ARTICLE INFO

Article history:
Received 1 November 2015
Received in revised form 8 January 2016
Accepted 31 January 2016
Available online 3 February 2016

Keywords:
Superparamagnetic
β-cyclodextrin (β-CD)
Fenton-like
4-Chlorophenol (4-CP)
Electron paramagnetic resonance (EPR)

ABSTRACT

The magnetic Fe_3O_4@β-cyclodextrin (β-CD) nanocomposites were fabricated via Fe ions and β-CD in one pot and characterized as a heterogeneous Fenton-like catalyst that may be used for the degradation of 4-chlorophenol (4-CP). The catalytic capacity of Fe_3O_4@β-CD was evaluated on the basis of various parameters, including pH, H_2O_2 concentration and catalyst loading, with regards to the pseudo-first-order kinetics of 4-CP degradation. In addition, iron leaching, the effect of radical scavengers and reusability of the Fe_3O_4@β-CD nanocomposite were also studied. The results showed that Fe_3O_4@β-CD exhibited a higher catalytic ability than that Fe_3O_4 toward 4-CP degradation, the observed rate constants (k_{obs}) were 0.0373 min^{-1} for Fe_3O_4@β-CD, and 0.0162 min^{-1} for Fe_3O_4, which may be ascribed to the construction of a ternary complex (Fe^{2+}–β-CD–pollutant) that allowed the produced hydroxyl radicals (·OH) to directly attack the contaminant and simultaneously enhanced the solubility of the organic pollutant. Fe_3O_4@β-CD also exhibited an enhancement effect for chlorobenzene (CB) degradation with the k_{obs} of 0.0392 min^{-1} (k_{obs} = 0.0099 min^{-1} for Fe_3O_4), which may be due to a synergistic effect in the Fe_3O_4@β-CD composite. Furthermore, Fe_3O_4@β-CD has an excellent catalytic activity, stable mechanical strength and adequate reusability. A possible reaction pathway of 4-CP degradation dominated by ·OH was proposed according to analyses of the degradation intermediates and chloride ions. The host-guest interaction between β-CD and 4-CP were examined with density functional theory (DFT) calculations, expounding the unicity of degraded intermediate owing to the specific spatial selectivity of β-CD. The findings of this study provide a novel material used in the Fenton-like process for the degradation of contaminants.

1. Introduction

Recently, advanced oxidation processes (AOPs) have been widely applied for the remediation of contaminated soil and water due to the increasing environmental concern [2,12,14,16]. Fenton reaction ($Fe^{2+} + H_2O_2 \rightarrow Fe^{3+} + OH^- + {}^{\bullet}OH$) is one of the most effective AOPs, which can generate hydroxyl radicals (•OH), the second strongest oxidizing agent after fluorine, and degrade pollutants efficiently [11,17,21]. The Fenton process has unique advantages, including its simple operation, mild reaction conditions, high degradation efficiency and inexpensive materials [9,30]. However, the traditional homogeneous Fenton reaction has some drawbacks; for example, (1) it is only efficient at low pH (pH 2–4) and is rather inefficient in most natural aqueous media (pH 5–9); (2) further treatments are required of the dissolved iron ions and sludge, such as neutralization of the treated solutions before discharge, which makes the Fenton process complex and uneconomical, and may even produce secondary pollution of acids or metal ions [13].

In order to overcome these problems, heterogeneous Fenton-like processes using iron-based catalysts have been recently studied extensively to decompose recalcitrant organic pollutants over a wider pH range with reduced iron loss [32]. Fenton-like oxidation mainly occurs at the solid–liquid interface, where the iron remains either in the solid phase or as an adsorbed ion [12]. Among the heterogeneous Fenton-like reactions, the inverse spinel Fe_3O_4 has been proved to be one of the most efficient catalyst, owing to its unique electric and magnetic properties [12,32]. The octahedral

* Corresponding author.
E-mail addresses: jhzhan@sdu.edu.cn, jhzhan@ustc.edu (J. Zhan).
[1] These authors contributed equally to this work and should be considered co-first authors.

http://dx.doi.org/10.1016/j.apcatb.2016.01.071

structure of magnetite can accommodate both Fe^{2+} and Fe^{3+}, allowing the iron species to be reversibly oxidized and reduced based on the transfer of electrons between Fe^{2+} and Fe^{3+} [12,32]. It can function steadily without substantial mass loss. Therefore, Fe_3O_4 provides a promising alternative due to its large specific surface, intrinsic peroxidase-like activity and its stability, as well as its facile recycling and recovery [1,33]. However, the solubility of hydrophobic organic pollutants is a vital factor for affecting the degradation of contaminants with Fenton-like reactions, since the contribution of hydroxyl radicals in aqueous solutions for contaminants degradation was also pivotal [24]. Thus, it is necessary to use a suitable enhancing agent that increases the solubility of organic pollutants and makes them available for oxidation.

β-Cyclodextrin (β-CD) is a cyclic oligosaccharide with seven glucose units and has been extensively employed in surface functionalization to promote the formation of host–guest inclusion complexes by providing a hydrophobic cavity, thus increasing the water solubility of organic pollutants [18,24,29]. The highly efficient absorption capacity of β-CD to some proper molecules is ascribed to its hydrophilic external surface, hydrophobic interior and specific cavity diameter (6.4 Å) via host–guest inclusion interaction [15]. The major advantages of using β-CD as an enhancing agent are (1) its much lower toxicity and higher biodegradability; (2) the lack of need for a critical micelle concentration and no formation of high viscosity emulsions, which minimizes reagent residuals; (3) the formation of a ternary pollutant–CD–iron complex, which allows direct ·OH radical attack of the contaminant, thus improving the pollutant elimination rate [34]. β-CD and its derivatives have been shown to be capable of enhancing the efficiency of Fenton oxidation [28]. Therefore, the combination of β-CD and Fe_3O_4 nanoparticles would facilitate the degradation of contaminants in the Fenton-like system.

In this paper, a β-CD-coated Fe_3O_4 catalyst was prepared in one pot and used to promote the Fenton oxidation of contaminant. 4-chlorophenol (4-CP) and chlorobenzene (CB) were selected as model pollutants, since they are widely used in the production of some herbicides, fungicides, insecticides and preservatives, and have been recorded as priority pollutants by the US Environmental Protection Agency (EPA) and European Decision 2455/2001/EC [20,22,27]. The physical and chemical properties of Fe_3O_4@β-CD composites were characterized and the catalytic performances were assessed according to the effects of key variables, such as pH, H_2O_2 concentration and catalyst dosage. The reaction kinetics, material stability and degradation mechanism were also evaluated.

2. Experimental

2.1. Chemicals

The chemicals used in this study are described in the Supporting information (SI, Text S1).

2.2. Preparation and characterization of Fe_3O_4@β-CD

The magnetic particles were prepared according to a previously reported simple one-pot method [3]. Briefly, $FeSO_4{\cdot}7H_2O$ (2.78 g) and $Fe_2(SO_4)_3$ (4 g) were dissolved in 25 mL H_2SO_4 aqueous solution (0.5 mol/L) with vigorous stirring under N_2. After 30 min stirring, 250 mL 4 mol/L NaOH solution (including 12.8 g β-CD) was added drop-wise. The reaction was conducted for 1.5 h with constant and vigorous stirring under N_2 at 80 °C. The obtained β-CD-modified Fe_3O_4 particles were washed several times with ethanol and deionized water, and dried in a vacuum at 60 °C for 6 h. Characterization of Fe_3O_4@β-CD is presented in SI Text S2.

2.3. Degradation experiments

Batch experiments were conducted in a conical flask (25 mL) placed on a rotary shaker at 100 rpm. The reaction solution was prepared by adding a required amount of catalyst to a solution containing the probe compound (4-CP) that was pH-adjusted in the range of 2.0–8.0 by addition of H_2SO_4 or NaOH. A known dosage of H_2O_2 was added to the suspension to initiate the reaction. The final concentration of H_2O_2 and catalyst loading were 10–50 mM and 0.5–2.0 g/L, respectively. Samples were taken at regular intervals and filtered through a 0.22 μm filter film and quenched with excess ethanol. The solid catalyst separated from the solution was rinsed with 2.5 mL methanol four times. The rinse liquid was collected and mixed for analysis. The amount of residual 4-CP was calculated from the sum of that in the aqueous and solid phases. The CB degradation experiments were conducted under the same reaction conditions as 4-CP degradation. The stability of the catalyst was evaluated by isolating it with a magnet, washing, drying under vacuum and reusing it for the next reaction under similar conditions.

2.4. Electron paramagnetic resonance (EPR) studies

5,5-Dimethyl-1-pyrroline-*N*-oxide (DMPO) was used as spin-trapping agent. The mixture for the standard EPR spin trapping experiment contained 1.0 g/L magnetic nanoparticles (MNPs) and 0.1 M DMPO. After completely mixing, the solution was analyzed by EPR. EPR spectra were also obtained with DMPO or MNPs alone. The spin trapping signals were recorded after 1 min. EPR spectra were also obtained for MNPs solutions in the presence of 10 mM ethanol, as well as MNPs solutions at different pH values after 1 min. Details of instrument are described in SI Text S3.

2.5. Analysis

Details about the analysis could be found in SI Text S4. 4-CP and CB degradation was described with pseudo-first-order equations: $\ln(C_0/C_t) = k_{obs}t$, where t is the reaction time (min), k_{obs} is the apparent rate constant (min^{-1}), and C_0 and C_t are 4-CP concentrations at times of $t = 0$ and $t = t$, respectively [23].

2.6. Computational details

Computational details are described in SI Text S5.

3. Results and discussion

3.1. Characterization of Fe_3O_4@β-CD

TEM images are shown in Fig. 1 and depict the morphology and particle size of Fe_3O_4, Fe_3O_4@β-CD and reused Fe_3O_4@β-CD. It can be observed that Fe_3O_4 and Fe_3O_4@β-CD are quasi-spherical and almost uniform, with diameters of 10–20 nm. The image of Fe_3O_4@β-CD composites reused three times (Fig. 1C) showed no obvious change after the oxidation reaction, which is in accordance with the results of XRD.

Fig. 1A displays the XRD patterns of Fe_3O_4 (top), Fe_3O_4@β-CD (middle) and reused Fe_3O_4@β-CD nanocomposites (bottom). Fe_3O_4 exhibited a spinel structure with five characteristic peaks, marked (2 2 0), (3 1 1), (4 0 0), (5 1 1) and (4 4 0). The intensity of the XRD peaks decreased when Fe_3O_4 particles were modifed with β-CD. However, Fe_3O_4 and Fe_3O_4@β-CD had similar diffraction peaks, indicating that β-CD did not affect the crystal structure of Fe_3O_4.

The FT-IR spectra of Fe_3O_4 (top), Fe_3O_4@β-CD (middle) and reused Fe_3O_4@β-CD nanocomposites (bottom) are given in Fig. 1B for comparison. The strong band at 570 cm^{-1} in the top trace is

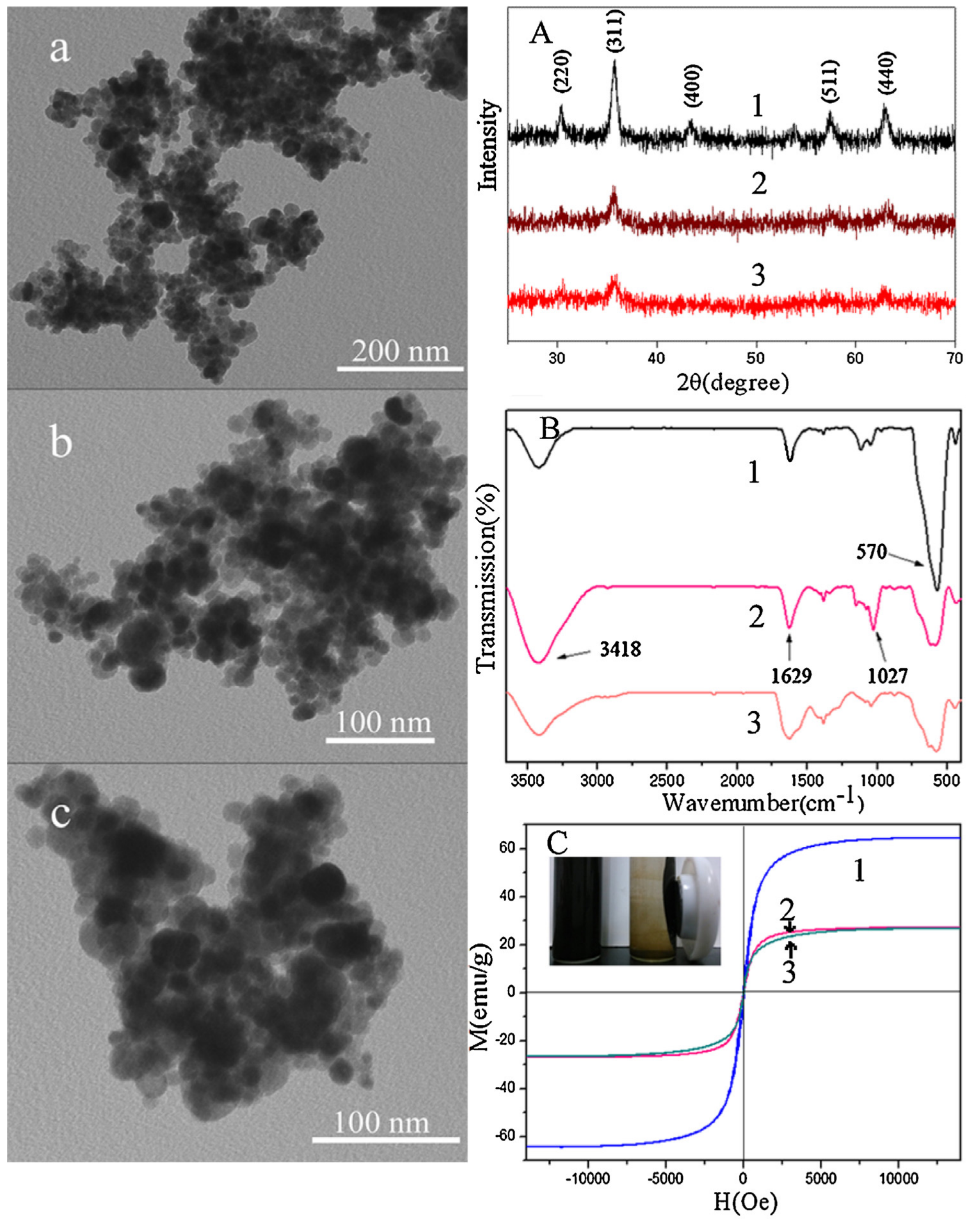

Fig. 1. (Left) TEM images of Fe_3O_4 (a), Fe_3O_4@β-CD (b) and reused Fe_3O_4@β-CD (c); (A) XRD patterns of Fe_3O_4 (1), Fe_3O_4@β-CD (2) and reused Fe_3O_4@β-CD (3); (B) FT-IR spectra of Fe_3O_4 (1) and Fe_3O_4@β-CD (2) and reused Fe_3O_4@β-CD (3); (C) Magnetization curves of Fe_3O_4 (1) and Fe_3O_4@β-CD (2) and reused Fe_3O_4@β-CD (3). Inset is a photo of the sample in solution (left) and attracted to a magnet (right).

the characteristic peak of Fe_3O_4 and is due to the Fe—O stretching vibration. The peaks around 1027 cm^{-1} and 3418 cm^{-1} in the middle trace can be assigned to the C—O and O—H stretching vibrations. The peak at 1629 cm^{-1} can be ascribed to the O—H in-plane bending vibration of β-CD. These peaks indicate the successful modification of β-CD on the Fe_3O_4 surface. The FT-IR spectrum of Fe_3O_4@β-CD composites reused three times showed similar peak location and height with unused Fe_3O_4@β-CD, which indicated the slight differences on Fe_3O_4@β-CD surface after the oxidation reaction.

Room temperature magnetization curves of Fe_3O_4 (top), Fe_3O_4@β-CD (middle) and reused Fe_3O_4@β-CD nanocomposites (bottom) are displayed in Fig. 1C. Almost no coercivity and remanence indicated the superparamagnetic properties, which are crucial for separation. The saturation magnetization values of Fe_3O_4, Fe_3O_4@β-CD and reused Fe_3O_4@β-CD were 64.43, 26.65 and 26.39 emu/g, respectively. The lower value of Fe_3O_4@β-CD was attributed to the nonmagnetic contribution of β-CD. The value of reused Fe_3O_4@β-CD was much close to that of unused Fe_3O_4@β-CD. The inset image in Fig. 1C shows the superparamagnetism visually, indicated by the composite being easily separated from solution by an external magnetic field.

3.2. *Catalytic properties of the Fe_3O_4@β-CD composite*

Batch experiments were performed to assess the catalytic ability of Fe_3O_4@β-CD for 4-CP degradation in the presence of 30 mM H_2O_2. As shown in Fig. 2, the 4-CP was completely disappeared within 90 min and 120 min in the Fe_3O_4@β-CD/H_2O_2 and Fe_3O_4/H_2O_2 systems, respectively. While the concentration of 4-CP changed slightly in H_2O_2, H_2O_2/β-CD and Fe_3O_4@β-CD alone. These results suggested that Fe_3O_4@β-CD exhibited an excellent catalytic ability toward H_2O_2 for 4-CP degradation. Rapid removal of 4-CP was achieved in heterogeneous Fenton-like reactions catalyzed by both Fe_3O_4 or Fe_3O_4@β-CD composites, implying that the

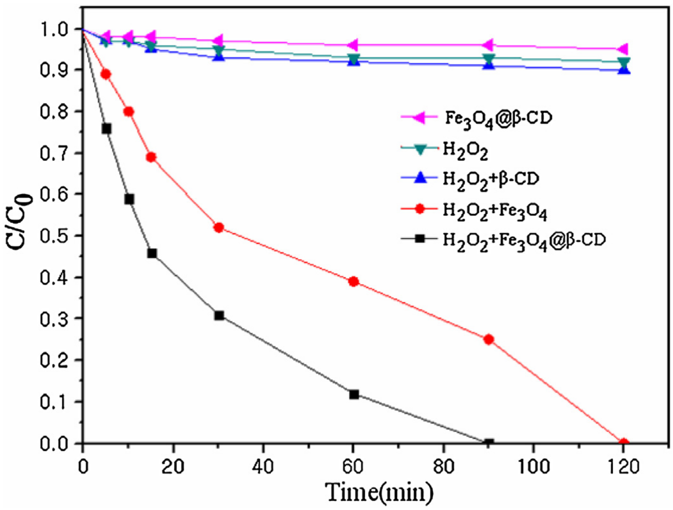

Fig. 2. Kinetics of 4-CP degradation in the different systems. Reaction conditions: $[4\text{-CP}]_0 = 100$ mg/L, $[H_2O_2]_0 = 30$ mmol/L, $[Fe_3O_4]_0 = 2$ g/L, $[Fe_3O_4@\beta\text{-CD}]_0 = 2$ g/L, $[\beta\text{-CD}]_0 = 20$ mg/L, pH 3 and 20 °C.

dissociation of H_2O_2 was mainly activated by Fe_3O_4. Furthermore, the degradation of 4-CP followed the pseudo-first-order equation, and observed rate constants (k_{obs}) were 0.0373 min^{-1}($R^2 = 0.98$) for $Fe_3O_4@\beta$-CD, and 0.0162 min^{-1}($R^2 = 0.98$) for Fe_3O_4, which indicated that $Fe_3O_4@\beta$-CD nanocomposite was more efficient than that Fe_3O_4 nanoparticles alone for 4-CP degradation. To further testify the enhancement an effect of Fe_3O_4 combined with β-CD for the catalytic degradation of contaminants, the $Fe_3O_4@\beta$-CD was applied to catalytic decomposes H_2O_2 for CB degradation. As shown in Fig. 3, $Fe_3O_4@\beta$-CD also exhibited an excellent catalytic ability for CB degradation with the k_{obs} of 0.0392 min^{-1}($R^2 = 0.99$), which was significantly higher than that Fe_3O_4 for CB degradation ($k_{obs} = 0.0099$ min^{-1}, $R^2 = 0.98$). The results further confirmed the enhancement effects of $Fe_3O_4@\beta$-CD on contaminants degradation.

The removal of 4-CP using $Fe_3O_4@\beta$-CD in the presence of H_2O_2 was evidently higher than that pure Fe_3O_4, which indicated that the catalytic efficiency was promoted by incorporation of β-CD, which may be due to a synergistic effect in the $Fe_3O_4@\beta$-CD composite. The proposed pathways for this process are described in Scheme 1. The $Fe_3O_4@\beta$-CD composite, which was water dispersable and stable, was synthesized via Fe ions and β-CD in one pot. Then, H_2O_2 was catalyzed by the $Fe_3O_4@\beta$-CD composites to generate hydroxyl radicals. Meanwhile, the hydrophobic organic pollutant was trapped in the β-CD cavity, resulting in the construction of a ternary complex (Fe^{2+}–β-CD–pollutant), which allowed the generated ·OH in proximity to β-CD to directly attack the contaminant. Therefore, a faster degradation rate of the pollutant can be achieved due to the formation of a ternary complex and the increase of local concentration of contaminant reactant within the β-CD cavity. The existence of such a ternary complex has previously been shown by liquid chromatography, electrospray-mass spectrometry, nuclear magnetic resonance (NMR) and fluorescence spectroscopy [17,21,28,34].

Furthermore, the enhancement effects verified significantly with different target contaminants. For 4-CP, the k_{obs} for $Fe_3O_4@\beta$-CD is 2.3 times as high as Fe_3O_4, while for CB, the k_{obs} for $Fe_3O_4@\beta$-CD is 4.0 times as high as Fe_3O_4. The likely reason for this behavior was that hydrophobic ability of these two compounds varied significantly, where 4-CP and CB were used as model molecules of mid-hydrophilic and hydrophobic organic compounds, respectively. Considering β-CD can increase the water solubility of organic compounds due to its hydrophilic external surface and hydrophobic interior, it is supposed that $Fe_3O_4@\beta$-CD

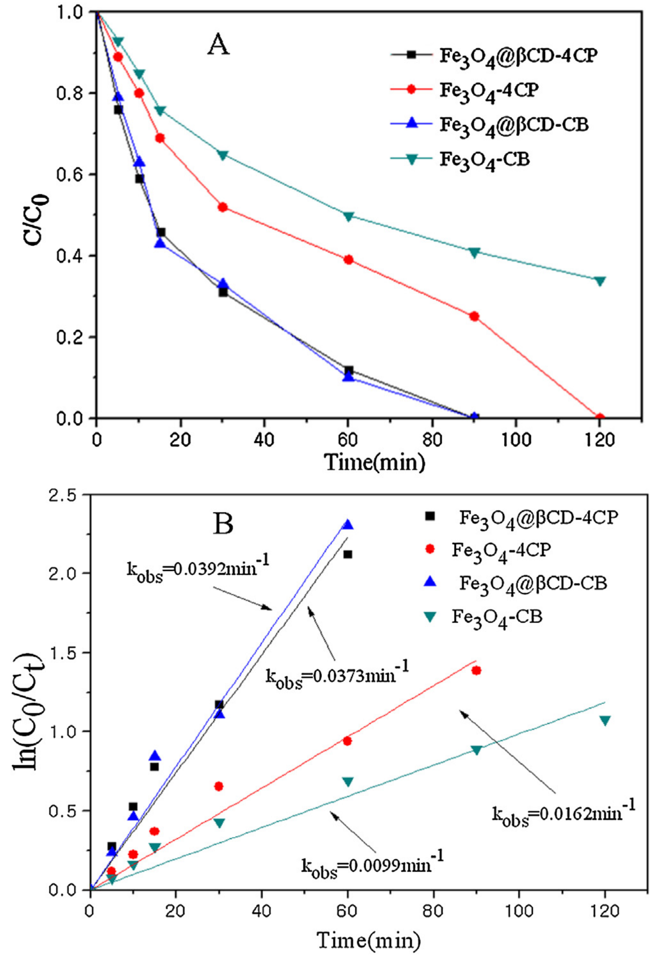

Fig. 3. Comparison of the degradation of 4-CP and CB with $Fe_3O_4@\beta$-CD and Fe_3O_4 in the presence of H_2O_2 (A) kinetics of 4-CP degradation by $Fe_3O_4@\beta$-CD and Fe_3O_4 with H_2O_2, and pseudo-first-order equation fitting for the kinetic data (B). Reaction conditions: $[4\text{-CP}]_0 = 100$ mg/L, $[CB]_0 = 87.5$ mg/L, $[H_2O_2]_0 = 30$ mmol/L, $[Fe_3O_4]_0 = 2$ g/L, $[Fe_3O_4@\beta\text{-CD}]_0 = 2$ g/L, pH 3, and 20 °C.

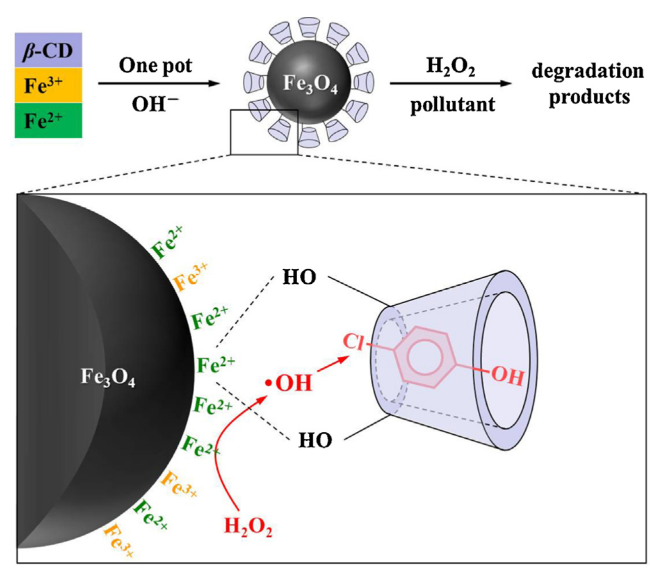

Scheme 1. Schematic diagram of the preparation of the $Fe_3O_4@\beta$-CD catalyst and the degradation process.

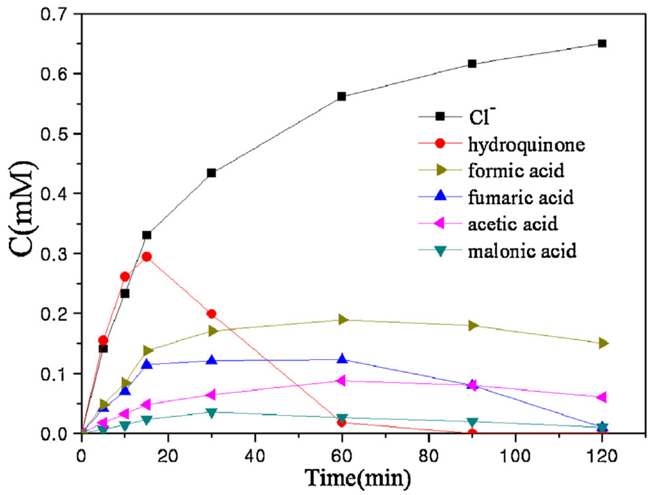

Fig. 4. Variation of the concentration of chloride ions and intermediates during the 4-CP degradation with Fe_3O_4@β-CD and H_2O_2. Reaction conditions:$[4\text{-}CP]_0 = 100$ mg/L, $[H_2O_2]_0 = 30$ mmol/L, $[Fe_3O_4@\beta\text{-}CD]_0 = 2$ g/L, pH 3 and 20 °C.

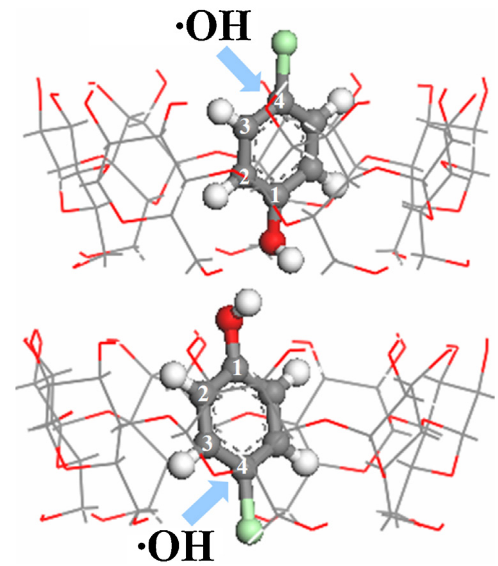

Fig. 5. The geometries of two inclusion complexes between β-CD and 4-CP.

has a higher efficiency to degrade organic compounds with sub-optimal solubility. Therefore, Fe_3O_4@β-CD was more efficient for hydrophobic contaminants than hydrophilic contaminants.

3.3. Possible pathways for 4-CP degradation

The degradation products of 4-CP was further determined. As seen in Fig. 4, the concentration of chloride ions increased from 0 to 0.66 mM with reaction time of 120 min, which accounted for about 84.6% of total Cl^- concentration of 4-CP mineralization (0.78 mM). The results indicated that some unknown chlorinated intermediates produced in the reaction system, which was supported by the TOC analysis that the TOC removal was only 56% with the reaction time of 120 min (Fig. S2). As a main aromatic intermediate, hydroquinone exhibited a peak concentration and then further decreased until complete removal. The aliphatic carboxylic acid intermediates were produced gradually and remained in solution.

According to the previous studies and experimental results observed in our study, a possible degradation pathway is proposed in Scheme 2 [22,32,33]. Because 4-chlorocatechol was not detected in our system, the ·OH addition to C(2) of 4-CP can be ignored. Firstly, the chlorine located in the *para* position of the aromatic ring was substituted by •OH to generate hydroquinone, which may be attributed to the steric effect of forming a ternary complex (Fe^{2+}–β-CD–pollutant), as mentioned in Section 3.2. Afterward, hydroquinone was dehydrogenated to give benzoquinone. The ring of benzoquinone was cleaved by attack of ·OH to yield aliphatic carboxylic acids, such as fumaric and malonic acid, which were converted into some smaller molecular organic acids that then remained in solution. Taking into account practical use, total degradation of 4-CP to CO_2 and H_2O is not necessary as biodegradable aliphatic carboxylic acids can be degraded through economical biological processes.

To better understand the degradation behavior of 4-CP initiated by ·OH, density functional theory (DFT) calculations were performed in Fig. 5. The geometries of two inclusion complexes both showed that the *para*-site of phenolic hydroxyl (C-4 site) had a smaller steric hindrance than the *ortho*-site (C-2 site). It may infer that •OH prefers to attack the C-4 than C-2 site, thus 4-chlorocatechol, the C-2 site product, was not detected in our system. As is known to all, polychlorinated dibenzo-*p*-dioxin/dibenzofurans (PCDD/Fs), the chlorinated species of extreme toxic and persist in the environment, have never been intentionally prepared or used and they are occurred as unwanted byproducts via the self- and cross-coupling condensation of chlorophenoxy radical, chlorinated phenyl radical and chlorinated α-ketocarbene during the general surface-catalyzed processes: the *de novo* route and precursor route, while chlorophenols are regarded as the key precursors [10,25,31,35]. However, in our system the C-2 site product was not detected due to the specific spatial selectivity of β-CD, which hindered the formation of *ortho*-site radical and condensation of several chlorophenolic radicals, further avoiding the generation of PCDD/Fs and finally decomposing into small biodegradable molecules.

3.4. Effects of pH, oxidation concentration and catalyst loading on 4-CP degradation

It has been well established that pH can notably influence the Fenton reaction for contaminants degradation [17,21,32,33]. The effect of pH on the degradation of 4-CP with Fe_3O_4@β-CD was examined. As shown in Fig. 6A, the k_{obs} increased markedly from 0.0052 min^{-1} to 0.0790 min^{-1} ($R^2_{pH8} = 0.82$, $R^2_{pH5} = 0.94$, $R^2_{pH3} = 0.98$, $R^2_{pH2} = 0.99$) as pH decreased from 8.0 to 2.0, which indicated that decrease pH favored the degradation of 4-CP in the Fe_3O_4@β-CD/H_2O_2 system. The catalytic reaction still occurred at neutral and alkaline solutions, suggesting that Fe_3O_4@β-CD would be used over a wide range of pH values for catalytic degradation of contaminants. The increased degradation efficiency of 4-CP at lower pH would be ascribed to the higher concentrations of Fe dissolved from Fe_3O_4@β-CD particles, which favored the generation of •OH though the homogeneous Fenton reactions. Furthermore, the lower of pH values, the higher oxidation potential of •OH was achieved, which favored the degradation of contaminants.

The degradation of 4-CP at different H_2O_2 concentrations was studied, as shown in Fig. 6B. It was observed that the k_{obs} for 4-CP degradation increased significantly from 0.0112 to 0.0373 min^{-1} ($R^2_{10mM} = 0.96$, $R^2_{20mM} = 0.99$, $R^2_{30mM} = 0.98$) with H_2O_2 concentration increased from 10 to 30 mM, indicating that the degradation of 4-CP was directly related to the concentration of ·OH radicals, which were produced from the reaction between H_2O_2 and Fe^{2+}. Moreover, H_2O_2 can also react with Fe^{3+} to regenerate Fe^{2+} ions, which then take part in the Fenton reaction again, thus increasing H_2O_2 concentration favored •OH generation and contaminants degradation. However, the k_{obs} ($R^2_{50mM} = 0.99$) of 4-CP degradation decreased markedly with an increase of H_2O_2 concentration up to

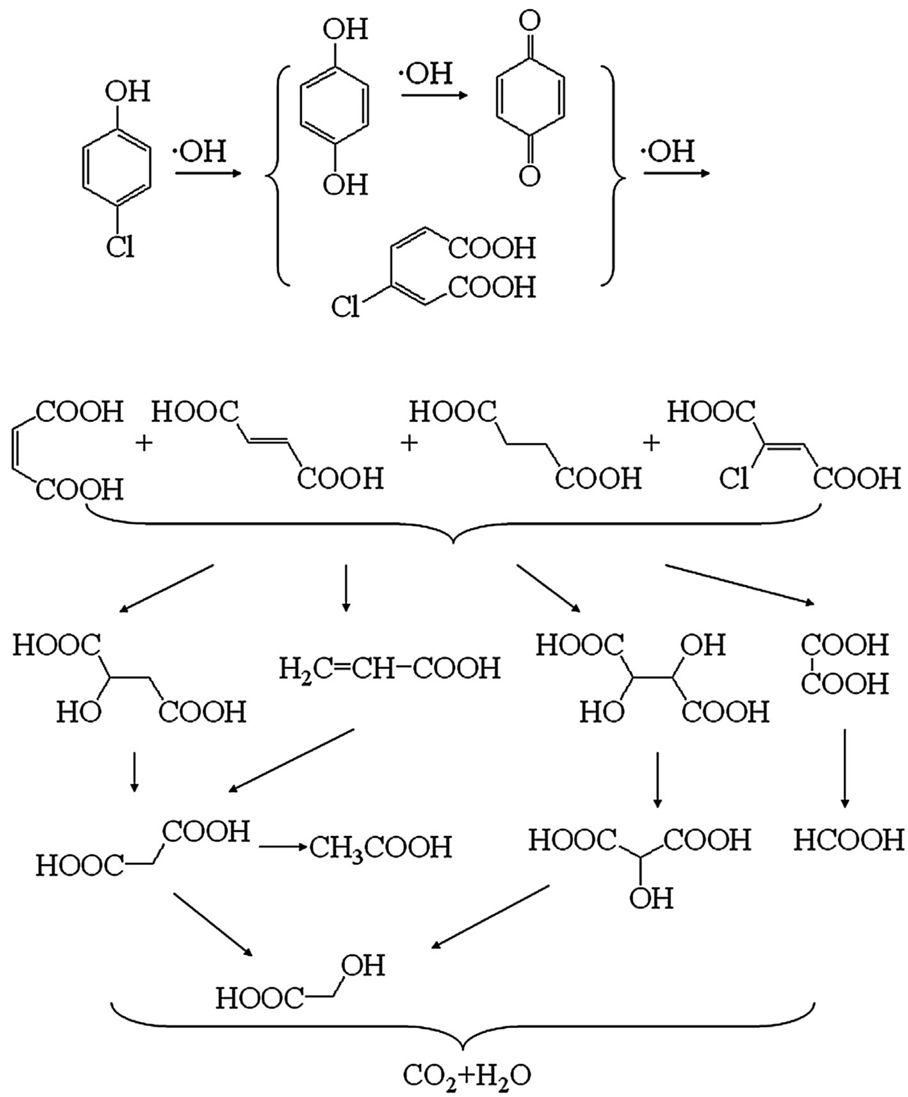

Scheme 2. Proposed pathway for 4-CP degradation with hydroxyl radical.

50 mM, which may possibly be attributed to the scavenging of $^{\bullet}OH$ and the inhibition of iron corrosion by H_2O_2 [33]. For an excessive H_2O_2 loading, there is a competitive reaction between 4-CP and H_2O_2 for the consumption of $^{\bullet}OH$, which limits the degradation of 4-CP. The $\cdot OH$ radicals can react with H_2O_2 to generate hydroperoxyl radicals ($^{\bullet}OOH$) and superoxide anions ($O_2^{\bullet -}$), as expressed by the following equations [12].

$$^{\bullet}OH + H_2O_2 \rightarrow H_2O + HOO^{\bullet} \tag{1}$$

$$HOO^{\bullet} \leftrightarrow O_2^{\bullet -} + H^{+} (pK_a 4.8) \tag{2}$$

Furthermore, $^{\bullet}OOH$ and $O_2^{\bullet -}$ have much lower oxidation potentials than $^{\bullet}OH$ and provide much less contribution to the degradation process.

Fig. 6C displays the 4-CP degradation with various loadings of Fe_3O_4@β-CD composites. The k_{obs} of 4-CP degradation increased rapidly from 0.0127 to 0.0373 min^{-1} ($R^2_{0.5g/L}$ = 0.98, $R^2_{0.7g/L}$ = 0.99, $R^2_{1.0g/L}$ = 0.98) with Fe_3O_4@β-CD loadings increased from 0.5 to 1.0 g/L, and then decreased to 0.0228 min^{-1} ($R^2_{2.0g/L}$ = 0.98) with further increased Fe_3O_4@β-CD loading up to 2.0 g/L. The likely reason was that the number of active sites increased as the increased Fe_3O_4@β-CD loadings, which acted as a peroxidase-like catalyst to accelerate the decomposition of H_2O_2 and the generation of $^{\bullet}OH$. Furthermore, the concentration of Fe dissolution from Fe_3O_4@β-CD particles increased with increasing Fe_3O_4@β-CD loadings, which also favored $\cdot OH$ generation and 4-CP degradation. However, the k_{obs} of 4-CP degradation decreased with increasing Fe_3O_4@β-CD loading up to 2.0 g/L, which probably due to that the excessive Fe_3O_4@β-CD MNPs reduced the unit surface adsorption of H_2O_2 on the catalyst surface under the optimum H_2O_2 concentration. Moreover, the catalytic reaction for 4-CP degradation was usually occurred on the surface of Fe_3O_4@β-CD MNPs, especially, on the H_2O_2 adsorbed surface. Thus, the excessive Fe_3O_4@β-CD MNPs could decrease the density of surface adsorbed H_2O_2, and reduce the concentration of $^{\bullet}OH$ on MNPs surface, and thereby decrease the degradation efficiency of 4-CP. Moreover, an excessive Fe_3O_4@β-CD composite concentration may result in the agglomeration of nanoparticles and the scavenging of $^{\bullet}OH$ or other radicals by iron species through the following equations [12,13,32,33].

$$^{\bullet}OH + Fe^{2+} \rightarrow OH^{-} + Fe^{3+} \tag{3}$$

$$HOO^{\bullet} + Fe^{2+} \rightarrow HOO^{-} + Fe^{3+} \tag{4}$$

$$HOO^{\bullet} + Fe^{3+} \rightarrow Fe^{2+} + O_2 + H^{+} \tag{5}$$

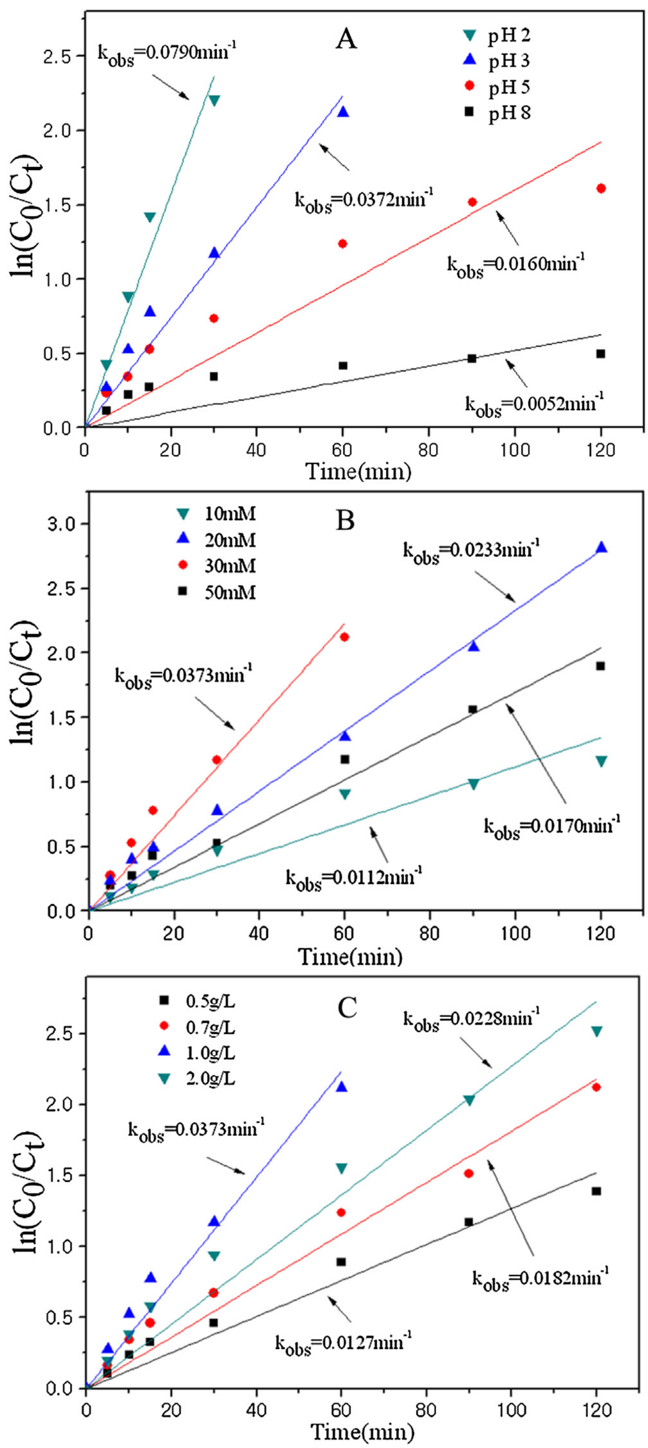

Fig. 6. (A) The effect of pH on 4-CP degradation ($[4\text{-CP}]_0 = 100$ mg/L, $[H_2O_2]_0 = 30$ mmol/L, $[Fe_3O_4@\beta\text{-CD}]_0 = 2$ g/L). (B) The effect of H_2O_2 concentration on 4-CP degradation ($[4\text{-CP}]_0 = 100$ mg/L, $[Fe_3O_4@\beta\text{-CD}]_0 = 2$ g/L, pH = 3). (C) The effect of $Fe_3O_4@\beta$-CD loading on 4-CP degradation ($[4\text{-CP}]_0 = 100$ mg/L, $[H_2O_2]_0 = 30$ mmol/L, pH 3).

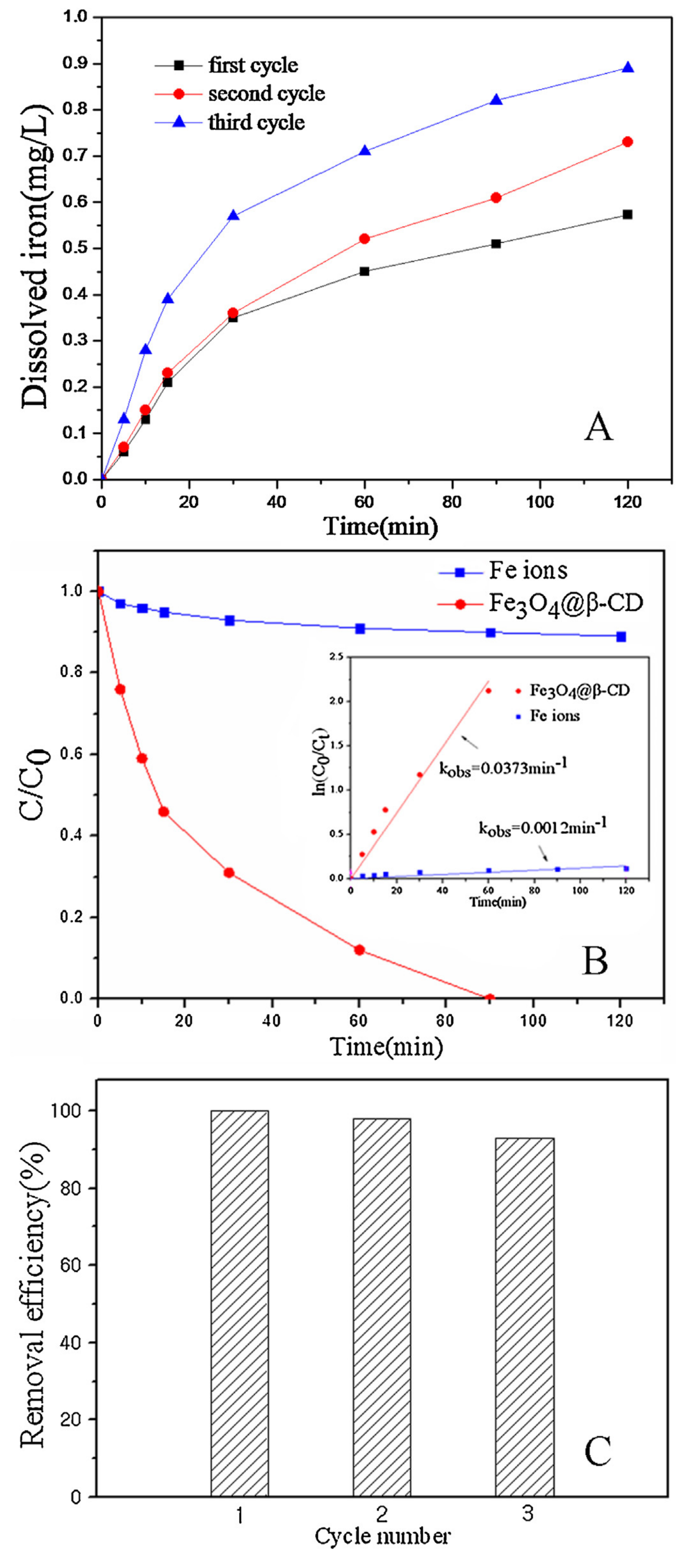

Fig. 7. (A) Iron leakage during 4-CP degradation in repeated experiments ($[Fe_3O_4@\beta\text{-CD}]_0 = 2$ g/L, $[H_2O_2]_0 = 30$ mmol/L, pH 3). (B) The effect of homogeneous and heterogeneous catalysis on 4-CP degradation. (C) Reusability of $Fe_3O_4@\beta$-CD for 4-CP degradation.

3.5. Stability and reusability of $Fe_3O_4@\beta$-CD

Minerals containing only Fe^{3+} or amorphous iron oxide may be less stable and more soluble on the catalyst surface. Therefore, the stability is a crucial characteristic of heterogeneous catalysts. Fe ions leaching from $Fe_3O_4@\beta$-CD were detected during the Fenton oxidation over three cycles. Fig. 7A shows that the leached total iron concentration increased from 0.6 to 1.0 mg/L as the cycle number increased. A similar phenomenon has been observed in previous studies [12,19,26]. This result may be attributed to the generation of incompatible and soluble iron (hydr) oxides during repeated oxidation.

In order to estimate the influence of dissolved Fe ions in solution on a homogeneous Fenton reaction, batch experiments were

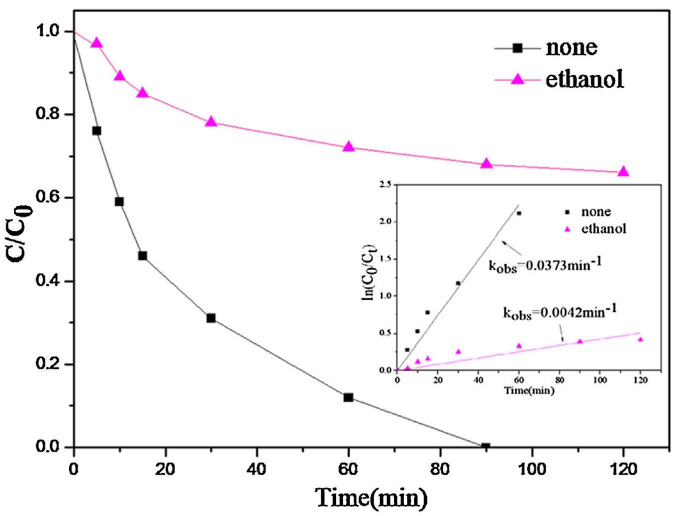

Fig. 8. Effect of radical scavengers on 4-CP degradation. Reaction conditions: $[4\text{-CP}]_0 = 100$ mg/L, $[H_2O_2]_0 = 30$ mmol/L, $[Fe_3O_4@\beta\text{-CD}]_0 = 2$ g/L, pH 3 and 20 °C.

conducted using iron salts in the same reaction condition based on the maximal amount of leached Fe ions. Fig. 7B shows that the 4-CP degradation efficiency was 9% after 1.5 h, implying that homogeneous catalysis provided only a very small contribution to the total 4-CP degradation ($R^2_{Fe3O4@\beta\text{-CD}} = 0.98$, $R^2_{Feions} = 0.87$). Therefore, H_2O_2 activation, namely the generation of •OH, was mainly ascribed to heterogeneous catalysis by $Fe_3O_4@\beta$-CD. Previous research has suggested that the dissolved iron species present in solution may include particulate iron oxyhydroxides, which are less soluble and possess very weak catalytic activity [12]. In general, the occurrence of the heterogeneous Fenton-like reaction and •OH production were mostly on the surface of the solid catalyst. In this way, the organics adsorbed on the catalyst surface may be attacked directly and degraded by •OH without the homogeneous Fenton pathway initiated by leached Fe ions. Thus, iron composites were recycled efficiently without great loss of ions into the solution.

Batch experiments were conducted to evaluate the reusability of $Fe_3O_4@\beta$-CD. As shown in Fig. 7C, it is clear that the initial degradation efficiency decreased slightly with the number of consecutive runs after 1.5 h under similar reaction conditions. This behavior was most likely due to the structural stability of magnetite chelating to β-CD and low-level iron leakage. As seen in the XRD pattern of reused $Fe_3O_4@\beta$-CD after three runs (Fig. 1A), no other peaks were observed. This implied that there was no obvious change to the structure and components of the catalyst after three cycles of the oxidation reaction. Previous research has suggested that catalyst deactivation was mainly attributable to factors including decrease of the catalyst specific area, poisoning of the active catalytic sites by adsorbed organic species, decay of active catalytic sites caused by leached active components, conglomeration of nanoparticles and mass loss due to the discarding of supernatants during rinsing [32,33].

3.6 •OH identification and proposed pathways for H_2O_2 activation

Free radical quenching studies are effective for the identification of reactive species in the Fenton or Fenton-like system. Therefore, ethanol was used as scavenger of •OH in $Fe_3O_4@\beta$-CD/H_2O_2. As shown in Fig. 8, the degradation of 4-CP was greatly inhibited by the addition of excess ethanol, indicating that the ·OH was the main reactive species for 4-CP degradation. Furthermore, the k_{obs} of 4-CP degradation decreased rapidly from 0.0373 min^{-1} ($R^2_{none} = 0.98$) to 0.0042 min^{-1} ($R^2_{ethanol} = 0.91$). These results indicated that •OH was the dominant reactive species for 4-CP degradation.

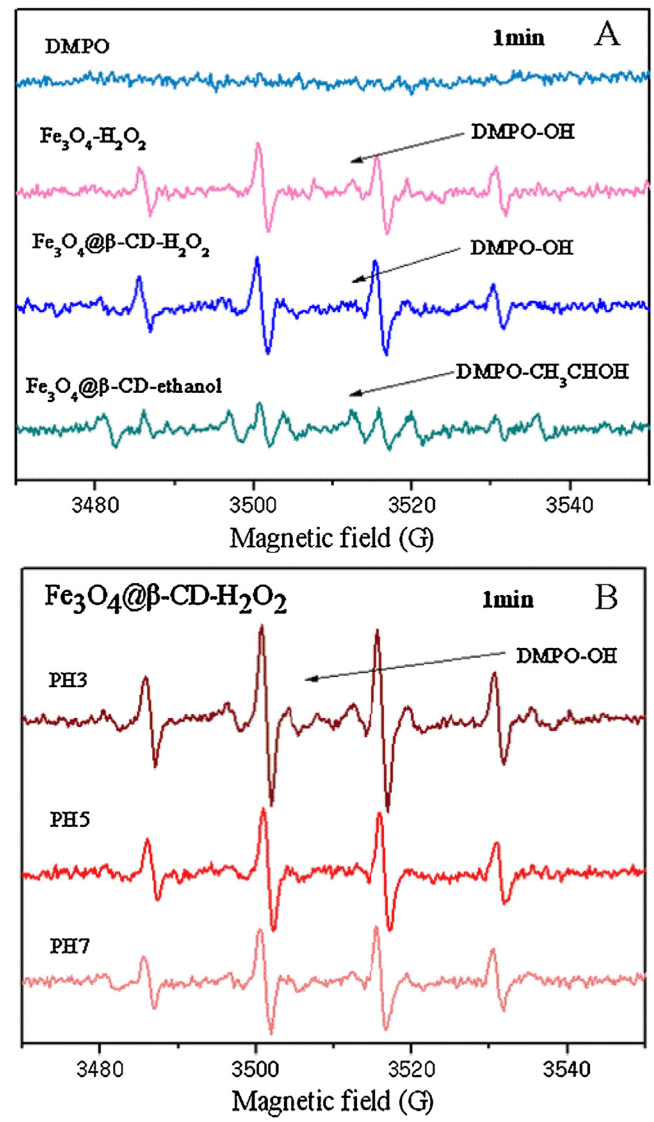

Fig. 9. DMPO spin-trapping EPR spectra of MNPs suspensions in the presence and absence of ethanol (a) The EPR spectra of MNPs at different pH (b) Reaction conditions: [MNPs] = 1.0 g/L, [ethanol] = 10 mM, [DMPO] = 0.1 M, pH 5, 25 °C and reaction time = 1 min.

To further identify radical species generated in the MNPs/H_2O_2 system, EPR plus coupled DMPO as the spin-trapping agent was used to detect ·OH radicals. As shown in Fig. 9A, the typical four characteristic peaks with an intensity ratio of 1:2:2:1 were obtained in the EPR spectra of Fe_3O_4/H_2O_2 and $Fe_3O_4@\beta$-CD/H_2O_2 in the presence of 0.1 M DMPO, while no signal was observed in pure DMPO solution. Their hyperfine splitting constants were consistent with the pattern of ·OH radicals added to DMPO, clearly indicating •OH generation from MNPs/H_2O_2 [5]. Furthermore, the peak intensities of DMPO–OH in the $Fe_3O_4@\beta$-CD/H_2O_2 system was slightly higher than that of Fe_3O_4/H_2O_2 system, which indicated that the scavenging influence of β-CD on the •OH radicals produced could be neglected using these MNPs. However, the DMPO–OH signal may also be observed due to other mechanisms, such as the reaction of Fe^{2+} and Fe^{3+} with DMPO or decomposition of DMPO–OOH. Therefore, ethanol was used as a scavenger to further confirm the existence of •OH radicals because ethanol can rapidly react with •OH to form •$CHCH_3OH$. If the DMPO–OH signal derived from trapped ·OH, efficient scavenging of •OH would generate a corresponding DMPO–$CHCH_3OH$ signal due to the new DMPO spin

adduct [6,8]. The DMPO–OH signal decreased greatly upon addition of 10 mM ethanol and a new EPR signal appeared, which was characteristic of $^{\bullet}CHCH_3OH$ radical DMPO adducts [4,7]. This indicated the formation of $^{\bullet}CHCH_3OH$ radicals by the reaction of $^{\bullet}OH$ and ethanol, further confirming the production of $^{\bullet}OH$ from H_2O_2 catalyzed by MNPs, while $^{\bullet}OH$ was mainly responsible for the degradation of chlorinated aromatics. Furthermore, Fig. 9B shows that the DMPO–OH signal decreased as the pH increased from 3.0 to 7.0, indicating that the $^{\bullet}OH$ concentration decreased as the pH increased. This could be attributed to the dissolved iron species from the MNPs being lower, yielding fewer $^{\bullet}OH$ at relatively high pH.

Based on literature and experimental results obtained here, a possible H_2O_2 activation mechanism by Fe_3O_4@β-CD can be proposed [12,32,33]. The process includes the redox cycle of Fe^{2+}/Fe^{3+}, both from the catalyst surface and the bulk solution. A complex assigned as $\equiv Fe^{2+} {}^{\bullet}H_2O_2$ is initially formed by ligand displacement between the hydrous surface of $\equiv Fe^{2+} {}^{\bullet}H_2O$ and H_2O_2, generating surface-bound $^{\bullet}OH_{ads}$ by intramolecular electron transfer, where $\equiv Fe^{2+} {}^{\bullet}H_2O$ stands for Fe^{2+} sites on the hydrous catalyst surface (Eq. (6), below). More $\equiv Fe^{2+}$ is produced via reduction of $\equiv Fe^{3+}$ species (Eqs. (7) and (8)). The dissolved iron species then diffuse into the bulk solution and initiate H_2O_2 decomposition through a chain reaction (Eqs. (13)–(15)). Furthermore, competitive reactions could occur, which negatively influence the Fenton process (Eqs. (16)–(19)). The ·OH radicals may be recombined or scavenged quickly by excess H_2O_2 and activated Fe_3O_4@β-CD composites before attacking the pollutants. Finally, 4-CP is degraded by $^{\bullet}OH$, both from the catalyst surface and the bulk solution.

$$\equiv Fe^{2+}{}^{\bullet}H_2O + H_2O_2 \rightarrow \equiv Fe^{2+}{}^{\bullet}H_2O_2 \rightarrow \equiv Fe^{3+} + {}^{\bullet}OH_{ads} + OH^- \quad (6)$$

$$\equiv Fe^{3+} + H_2O_2 \rightarrow \equiv Fe^{3+}{}^{\bullet}H_2O_2 \rightarrow \equiv Fe^{2+} + HOO^{\bullet} + H^+ \quad (7)$$

$$\equiv Fe^{3+} + HOO^{\bullet} \rightarrow \equiv Fe^{2+} + O_2 + H^+ \quad (8)$$

$$^{\bullet}OH_{ads} + H_2O_2 \rightarrow HOO^{\bullet} + H_2O \quad (9)$$

$$Fe^{2+} + H_2O_2 \rightarrow Fe^{3+} + {}^{\bullet}OH_{free} + OH^- \quad (10)$$

$$Fe^{3+} + H_2O_2 \rightarrow Fe^{2+} + HOO^{\bullet} + H^+ \quad (11)$$

$$Fe^{3+} + HOO^{\bullet} \rightarrow Fe^{2+} + O_2 + H^+ \quad (12)$$

$$^{\bullet}OH + Fe^{2+} \rightarrow OH^- + Fe^{3+} \quad (13)$$

$$^{\bullet}OH + H_2O_2 \rightarrow H_2O + HOO^{\bullet} \quad (14)$$

$$HOO^{\bullet} + Fe^{2+} \rightarrow HOO^- + Fe^{3+} \quad (15)$$

$$HOO^{\bullet} + HOO^{\bullet} \rightarrow H_2O_2 + O_2 \quad (16)$$

$$^{\bullet}OH + HOO^{\bullet}(O_2^{\bullet -}) \rightarrow O_2 + H_2O(+OH^-) \quad (17)$$

$$^{\bullet}OH + {}^{\bullet}OH \rightarrow H_2O_2 \quad (18)$$

$$^{\bullet}OH + 4\text{-CP} \rightarrow \text{degradedproducts} \quad (19)$$

7. Conclusions

In this study, β-CD-modified Fe_3O_4 magnetic nanoparticles (Fe_3O_4@β-CD) were prepared via one-pot synthesis from Fe ions and β-CD. The resulting composite was used as a heterogeneous Fenton-like catalyst to efficiently adsorb and degrade 4-CP in aqueous solution. The kinetic rates of 4-CP degradation depended on the pH, H_2O_2 concentration and catalyst dosage. We also investigated iron leaching, the effect of radical scavengers and the reusability of the Fe_3O_4@β-CD composites, as well as a comparison of the enhanced coefficient. Fe_3O_4@β-CD exhibited a higher catalytic ability than that of Fe_3O_4 toward H_2O_2 decomposition for 4-CP degradation. The observed rate constants (k_{obs}) were 0.0339 min^{-1} for Fe_3O_4@β-CD, and 0.0148 min^{-1} for Fe_3O_4. It also displayed an obvious enhancement effect for chlorobenzene (CB) degradation with the k_{obs} of 0.0370 min^{-1}, which was significantly higher than that of Fe_3O_4 for CB degradation (k_{obs} = 0.0088 min^{-1}). The increased catalytic activity in the presence of Fe_3O_4@β-CD composites may be attributed to the formation of a ternary complex (Fe^{2+}–β-CD–pollutant) and the resulting solubility of the organic pollutant. According to the intermediates and chloride ions released during degradation, a possible degradation pathway was proposed. The host-guest interaction between β-CD and 4-CP were further examined with density functional theory (DFT) calculations, expounding the unicity of degraded intermediate owing to the specific spatial selectivity of β-CD. Thus, Fe_3O_4 nanoparticles modified with cyclodextrins could be further explored due to their potential application in the treatment of contaminants in the future.

Acknowledgments

This work was supported by grants from the National Basic Research Program of China (973 Program 2013CB934301 and 2013CB934303), the National Natural Science Foundation of China (NSFC 21377068 and 21575077) and Shandong Provincial Natural Science Foundation for Distinguished Young Scholar (2010JQE27013).

Appendix A. Supplementary data

Supplementary data associated with this article can be found, in the online version, at http://dx.doi.org/10.1016/j.apcatb.2016.01.071.

References

[1] J. Ashby, S. Pan, W. Zhong, ACS Appl. Mater. Interfaces 6 (2014) 15412–15419.
[2] W.R.P. Barros, T. Ereno, A.C. Tavares, M.R.V. Lanza, Chemelectrochem 2 (2015) 714–719.
[3] X. Chen, J. Rao, J. Wang, G. Zou, Q. Zhang, Chem. Commun. 47 (2011) 10317–10319.
[4] G.D. Fang, D.D. Dionysiou, S.R. Al-Abed, D.M. Zhou, Appl. Catal. B: Environ. 129 (2013) 325–332.
[5] G.D. Fang, D.D. Dionysiou, Y. Wang, S.R. Al-Abed, D.M. Zhou, J. Hazard. Mater. 227–228 (2012) 394–401.
[6] G.D. Fang, J. Gao, C. Liu, D.D. Dionysiou, Y. Wang, D.M. Zhou, Environ. Sci. Technol. 48 (2014) 1902–1910.
[7] G.D. Fang, D.M. Zhou, D.D. Dionysiou, J. Hazard. Mater. 250–251 (2013) 68–75.
[8] G.D. Fang, C. Zhu, D.D. Dionysiou, J. Gao, D.M. Zhou, Bioresour. Technol. 176 (2015) 210–217.
[9] M. Fukushima, K. Tatsumi, K. Morimoto, Environ. Sci. Technol. 34 (2000) 2006–2013.
[10] Z. Han, D. Zhang, Y. Sun, C. Liu, Chem. Phys. Lett. 474 (2009) 62–66.
[11] D.Q. He, L.F. Wang, H. Jiang, H.Q. Yu, Chem. Eng. J. 272 (2015) 128–134.
[12] X. Hu, B. Liu, Y. Deng, H. Chen, S. Luo, C. Sun, P. Yang, S. Yang, Appl. Catal. B: Environ. 107 (2011) 274–283.
[13] R. Huang, Z. Fang, X. Yan, W. Cheng, Chem. Eng. J. 197 (2012) 242–249.
[14] S. Kawano, T. Kida, K. Miyawaki, Y. Noguchi, E. Kato, T. Nakano, M. Akashi, Environ. Sci. Technol. 48 (2014) 8094–8100.
[15] J. Li, C. Chen, Y. Zhao, J. Hu, D. Shao, X. Wang, Chem. Eng. J. 229 (2013) 296–303.
[16] Y. Li, Y. Huang, J. Cui, C. Jing, Water Res. 68 (2015) 572–579.
[17] M.E. Lindsey, G. Xu, J. Lu, M.A. Tarr, Sci. Total Environ. 307 (2003) 215–229.
[18] P. Liu, D. Zhang, J. Zhan, J. Phys. Chem. A 114 (2010) 13122–13128.
[19] J.A. Melero, G. Calleja, F. Martinez, R. Molina, M.I. Pariente, Chem. Eng. J. 131 (2007) 245–256.
[20] B. Meunier, Science 296 (2002) 270–271.
[21] E. Mousset, N. Oturan, E.D.V. Hullebusch, G. Guibaud, G. Esposito, M.A. Oturan, Water Res. 48 (2014) 306–316.
[22] M. Munoz, Z.M.D. Pedro, J.A. Casas, J.J. Rodriguez, Chem. Eng. J. 228 (2013) 646–654.
[23] H. Niu, Z. Di, S. Zhang, X. Zhang, Z. Meng, Y. Cai, J. Hazard. Mater. 190 (2011) 559–565.
[24] A. Oonnittan, R.A. Shrestha, M. Sillanpaa, Sep. Purif. Technol. 64 (2009) 314–320.
[25] W. Pan, D. Zhang, Z. Han, J. Zhan, C. Liu, Environ. Sci. Technol. 47 (2013) 8489–8498.
[26] J.H. Ramirez, F.J. Maldonado-H, A.F. Perez-Cadenas, C. Moreno-Castilla, C.A. Costa, L.M. Madeira, Appl. Catal. B: Environ. 75 (2007) 312–323.

[27] G. Sayam Sen, S. Matthew, C.A. Noser, G. Anindya, S. Bradley, L. Dieter, C.P. Horwitz, S. Karl-Werner, T.J. Collins, Science 296 (2002) 326–328.
[28] E. Veignie, C. Rafin, D. Landy, S. Fourmentin, G. Surpateanu, J. Hazard. Mater. 168 (2009) 1296–1301.
[29] M. Wang, P. Liu, Y. Wang, D. Zhou, C. Ma, D. Zhang, J. Zhan, J. Colloid Interface Sci. 447 (2015) 1–7.
[30] Q. Wang, A.T. Lemley, Environ. Sci. Technol. 35 (2001) 4509–4514.
[31] F. Xu, Wanni. Yu, R. Gao, Qin. Zhou, Q.Z. Zhang, W.X. Wang, Environ. Sci. Technol. 44 (2010) 6745–6751.
[32] L. Xu, J. Wang, Appl. Catal. B: Environ. 123–124 (2012) 117–126.
[33] L. Xu, J. Wang, Environ. Sci. Technol. 46 (2012) 10145–10153.
[34] G. Yardin, S. Chiron, Chemosphere 62 (2006) 1395–1402.
[35] Q.Z. Zhang, S. Li, X. Qu, X. Shi, W.X. Wang, Environ. Sci. Technol. 42 (2008) 7301–7308.